ACS OMEGA

http://pubs.acs.org/journal/acsodf

Article

Evaluation of Corrosion Inhibition of Essential Oil-Based Inhibitors on Aluminum Alloys

Omotayo Sanni,* Samuel A. Iwarere, and Michael O. Daramola*

Cite This: *ACS Omega* 2022, 7, 40740−40749

Read Online

ACCESS | Metrics & More | Article Recommendations

ABSTRACT: There is a high demand for eco-friendly, effective, and high-performance corrosion inhibitors for industrial applications. Thus, the corrosion property of aluminum alloys was studied in essential oil-containing sodium chloride solution at various concentrations. Potentiodynamic polarization, electrochemical impedance spectroscopy (EIS), surface tests, and weight loss analysis were used to study the corrosion inhibition mechanism of the essential oil. The essential oil showed the highest inhibition efficiency of 97.01% at 1000 ppm. A high efficiency of 96.03% was achieved even after 168 h of exposure. The potentiodynamic polarization test showed that the essential oil is a mixed-type inhibitor. EIS results show better adsorption of the oil on the surface of the aluminum at increased inhibitor concentrations. The Langmuir's adsorption isotherm model was found to describe the adsorption behavior. The surface morphology of the uninhibited and inhibited specimens examined by a scanning electron microscope equipped with an energy-dispersive X-ray spectroscope confirmed the protective film of the inhibitor molecules on the aluminum surface.

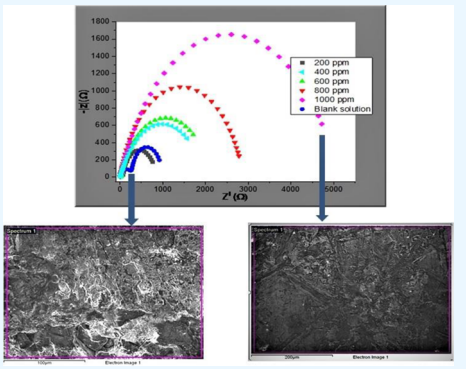

1. INTRODUCTION

Corrosion is a vital issue that has to be addressed by engineers and scientists working in the field of engineering and corrosion discipline globally because of its hazardous effects in various manufacturing industries. Aluminum is the second most used material for engineering application. The constant growth in consumption of aluminum, particularly in the packaging, transport, and engineering fields, can be ascribed to its outstanding properties: low density, easy recycling, attractive appearance, and so on. Because of the rapid advancement of industrial applications such as offshore platforms and direct current transmission, the aluminum alloy demand is rising.

Nevertheless, corrosion of aluminum alloys is a serious problem that causes severe environmental risks and economic losses, especially in the cooling systems.[1] The good corrosion resistance of pure aluminum is because of the spontaneous compact formed and adherent oxide films. Nevertheless, the surface layers contain much heterogeneity, such as intermetallic particles in the case of aluminum alloys. These intermetallic particles form local cathodes or anodes in the material microstructure and therefore increase the vulnerability for localized corrosion,[2,3] thus, making corrosion protection of aluminum alloys a serious subject. There are two major means of improving the corrosion resistance of aluminum alloys: (i) modification of the surface and (ii) tailoring the microstructure and composition. With notable progress recently, alloying is still a challenge because it does not allow long-lasting improvement in corrosion resistance. Therefore, the use of environmentally friendly and efficient protective schemes is of high importance.

Among the various available methods such as anodic/cathodic protection, corrosion-resistant materials, corrosion inspection, and monitoring tools, protective coatings, and corrosion inhibitors used fiercely for diverse applications in protecting metallic structures from corrosion, one of the most cost-efficient and popular approaches for corrosion control is the use of an inhibitor.[4,5] The inhibitor forms a protective film over the metal surface that separates the metal from destructive solutions and thus inhibits corrosion. The protective actions of the conventional inhibitors are based on the direct metallic surface passivation or interactions with the metal corrosion product, which results in passivation layer formation. For decades, hexavalent chromium has been applied mostly in protecting aluminum alloys from corrosion,[6,7] and this has caused pollution of the surrounding ecology of different industries, body implants, and so on.[8−10] thereby, making the replacement of these toxic compounds with environmentally benign substitutes desirable. Thus, the development of

Received: January 26, 2022
Accepted: March 14, 2022
Published: November 4, 2022

environmentally friendly and effective inhibitor alternatives has recently been given attention. In this context, the plant extracts from diverse parts of plants such as fruit, root, leaf, bark, stem, and peel have been used extensively as efficient corrosion inhibitors for numerous materials in several electrolytic solutions because of their biodegradability, versatility, renewability, biocompatibility, low cost, reliability, and simplicity. Phytochemicals with different heteroatoms for instance sulfur, nitrogen, and oxygen in the form of heterocyclic rings and polar groups have been extensively examined for corrosion inhibition.[11−15] Essential oils are more promising owing to their low toxicity, from the environmental viewpoint. In recent years, numerous authors[16−21] reported that essential oils can displace chloride ions from the solution−metal interface because of the competitive adsorption, and these adsorbed layers act as defensive barriers. Dahmani et al.[22] reported the importance of cinnamon essential oil in suppressing the cathodic activity of copper in acidified sodium chloride (NaCl) solution. The authors reported the highest efficiency of 89% at 200 ppm. Chraka et al.[23] also reported *Ammi visnaga* (L.) Lam essential oil harvested at different years for brass in sodium chloride solution, and an optimum efficiency of 96.36% was reported with 2 g/L concentration of the essential oil harvested in 2018. The inhibitive effect of most inhibitors in aggressive solution has been reported to depend on inhibitor concentration. The new perspective is expanding the eco-friendly and inexpensive corrosion inhibitors. The significant inhibitive behavior of sustainable corrosion inhibitors of plant extracts for metal corrosion in acidic environments has been examined by different researchers.[24−27] However, most of these inhibitors do not give a notable inhibitive performance in neutral saline solutions. Only few studies have demonstrated good inhibitive performance in saline solutions, until now. Selehi et al.[28] investigated the inhibitive behavior of *Nettle* leaf extracts in the chloride solutions on mild steel and established that the inhibitor molecules like histamine, quercetin, serotonin, and caffeic acid can offer promising corrosion inhibition because of the multitude of corrosion inhibitive compounds that exist in the inhibitor structure. The corrosion inhibitive behavior of the *Cichoriumintybus* L extracts was proved by Sanaei et al.[29] The inhibitive performance for *Nettle* leaves and *Cichoriumintybus* L extract was 51 and 26%, respectively. It is well known that the majority of natural inhibitors are inefficient in chloride solutions except with the addition of inorganic inhibitors.[28] Though some authors reported some natural compounds as efficient inhibitors for different metals in diverse environments, most of these inhibitors are not cost-effective and readily available. Therefore, using them for industrial applications would not be economically acceptable. Hence, while choosing an appropriate inhibitor for specific applications, some factors such as cost, high inhibition efficiency, the safety of the environment, and easy availability must be considered. Furthermore, the importance of aluminum corrosion in the chloride environment is related to its industrial application in recirculating water systems and heat exchangers. Also, it is significant to note that aluminum corrosion causes safety issues, huge economic losses, and energy losses. Thus, it is obligatory to examine the corrosion inhibition of aluminum in the chloride media. Despite the broad knowledge of corrosion inhibition of essential oils, the implementation of essential oils in inhibiting aluminum alloys is still scarce.

To overcome the problems arising from organic compounds, scientists have turned to using some essential oils as corrosion inhibitors for engineering materials in aggressive solutions. These natural oils are safe, harmless to humans, environmentally friendly, and economically viable when compared to other compounds. They are also characterized by containing effective compounds and groups that have a high adsorption capacity on the metal surfaces and give high inhibition efficiency.[48] Essential oils from plants have been known to act as natural additives, for instance, antioxidants, antimicrobial agents, and so on. Because of the unique smell associated with the volatiles, this may limit the use of essential oils in some foods because it may alter the typical smell/flavor of foods. However, film or packaging may have the smell of essential oils because of their volatilization.[50] The smell intensity of essential oils in films increased with increasing essential oil levels. This might limit the application of the film in food when incorporated at a high amount. However, a smaller amount (25%) of essential oil added did not cause a detrimental effect on smell perception or unacceptability of the film.[49,50] Active film-containing essential oil can be applied to extend the shelf life and maintain the quality of foods. Films can serve as carriers for various antimicrobial agents and antioxidants that can maintain fresh quality, extend product shelf life, and reduce the risk of pathogen growth.

Parsley is a medicinal plant with various proven pharmacological properties including antioxidant, antibacterial, and antifungal activities. Parsley components used as food additives will increase the antioxidant and antimicrobial potential of the food which prevent food deterioration and improve the shelf life of food besides its nutritional value.[51] It was found that the major volatile aroma constituent of parsley essential oil, myristicin, may be an effective cancer chemo-preventive agent. These observations encourage using parsley as a natural preservative agent which prevents food deterioration and improves the shelf life of food. Green corrosion inhibitors have a promising future for the quality of the environment because they do not contain heavy metals or other toxic compounds. In addition, they are biodegradable and renewable sources of materials. The biodegradable coating of parsley essential oil[52] has been extensively reported and represented as a sustainable and environmentally acceptable solution for primary packaging in the food industry, with the potential to be used on a commercial scale. Therefore, the choice of parsley essential oil is a result of its inhibitory action which could be linked with various factors such as the molecular structure, adsorption ability, and distribution of molecules on the metallic surface. The encouraging results obtained from previous studies and as part of the author's contribution to the growing interest in environmentally friendly corrosion inhibitors, the present work reports the corrosion inhibitive properties of parsley essential oil for aluminum corrosion in simulated seawater 3.5% NaCl solutions. To the best of the author's knowledge, an attempt to investigate the corrosion protection of aluminum alloys using parsley essential oil at the studied concentrations in 3.5% NaCl solutions has not been described in the literature. Therefore, this study aims to elucidate the corrosion inhibitive mechanism of parsley essential oil in simulated seawater 3.5% NaCl solution. Electrochemical analyses and surface studies are used in interpreting the essential oil inhibition mechanism in the chloride solutions.

2. EXPERIMENTAL SECTION

2.1. Materials and Chemicals. Type AA6063-T5 aluminum sheets with a purity of 97.87% as specified by the

https://doi.org/10.1021/acsomega.2c00540
ACS Omega 2022, 7, 40740−40749

manufacturer were utilized as a test material in this study for surface and electrochemical tests in 3.5 wt % sodium chloride media. The specimens were pressed-cut mechanically into samples of dimension 20 mm by 40 mm with 0.14 cm thickness. For rinsing and solution preparation, the Milli-Q Direct water (resistivity 18 MΩ cm) was used. Electrochemical measurements and surface analysis were conducted in 3.5 wt % NaCl solutions (99.7%, Fisher Scientific, Hampton, NH, USA), with a pH of ∼5.5. The samples were prepared, degreased, and cleaned as described previously.[30] All reagents and chemicals used were of analytical grade. The aggressive solution was prepared by dissolving the sodium chloride in the Milli-Q Direct water, signifying artificial seawater. The corrosive media have been used widely for testing aluminum corrosion resistance. The inhibitor test solution was prepared in the concentration range of 200, 400, 600, 800, and 1000 ppm parsley oil (PEO), respectively,[46] and the tests were conducted three times with approximately 99% reproducibility.

2.2. Testing Methods. *2.2.1. Electrochemical Tests.* Electrochemical tests were carried out at room temperature using three-electrode conventional corrosion cells. The working electrodes (aluminum alloy) were embedded in a resin with 1 cm^2 exposed area. A platinum rod was employed as a counter electrode while an Ag/AgCl electrode served as a reference electrode. The electrochemical experiment was conducted using a potentiostat/galvanostat Autolab PGSTAT30 (MetrohmAutolab, Utrecht, Netherlands) connected with NOVA 2.1 software. The electrode was first stabilized for 1 h to attain quasi-equilibrium values at an open circuit potential. From the current density vs potential line fitted slope, the polarization resistance (R_p) was determined using the NOVA software. Electrochemical corrosion data, corrosion current density (i_{corr}) and potentials (E_{corr}), were estimated from the polarization curve by Tafel approximation.

2.2.2. Electrochemical Impedance Spectroscopy (EIS). The potentiostat−galvanostat Autolab-PGSTAT30 and a frequency response analyzer were utilized with a Faraday cage to evade external interference. The conventional EIS three-electrode setup as described in Section 2.2.1 was used. The EIS test conditions were chosen to facilitate stability, linearity, and causality of the test to ensure reliable parameters. The result from the EIS was fitted with electrical equivalent circuits for differentiating the different stages of the protection/corrosion mechanism, and NOVA software was used for defining the system parameter characteristics. The Bode and Nyquist fitting relative errors were calculated according to.[31]

$$E_{error}(\%) = \frac{X_{measured} - X_{fit}}{X_{measured}} 100 \quad (1)$$

where X is each one of the (Z^I, Z^{II}, |Z|, and phase) parameters.

The EIS range at definite immersion time was fitted to one equivalent circuit per time.

2.2.3. Weight Loss Test. The cleaned aluminum samples were weighed, before immersion into the chloride solutions, with 0, 200, 400, 600, 800, and 1000 ppm PEO, for 168 h. The samples were cleaned following the ASTM standards[32] and reweighed. The tests were conducted three times, with approximately 99% reproducibility. The test sample preparation and experimental process for electrochemical, surface, and weight loss techniques were related to the one reported in the literature.[33] Equations 2 and 3 were employed to evaluate the corrosion rate (CR) and percentage inhibition efficiency at different inhibitor concentrations, respectively.

$$CR = \frac{87.6W}{D \times A \times T} \quad (2)$$

where T is the exposure time (hour), D is density (g/cm^2), A is area (cm^2), and W is weight loss (mg).

$$IE(\%) = \frac{CR_{(uninhibited)} - CR_{(inhibited)}}{CR_{uninhibited}} \times 100 \quad (3)$$

where $CR_{uninhibited}$ and $CR_{inhibited}$ are the corrosion rate in the absence and presence of an inhibitor, respectively.

2.2.4. Surface Analysis. Surface analysis was conducted on exposed samples for 168 h immersion in uninhibited and inhibited solutions using the backscattered electron signals recorded with a JEOL JSM-7600F microscope (Peabody, MA, USA) with a probe current of approximately 700 nA and 15 kV accelerating voltage. A scanning electron microscope equipped with energy-dispersive X-ray spectroscopy (EDX) was used for determining the elemental compositions on the sample surface.

3. RESULTS

3.1. Electrochemical Studies. *3.1.1. Potentiodynamic Polarization Tests.* The polarization curve for the uninhibited and inhibited aluminum specimens is shown in Figure 1. The

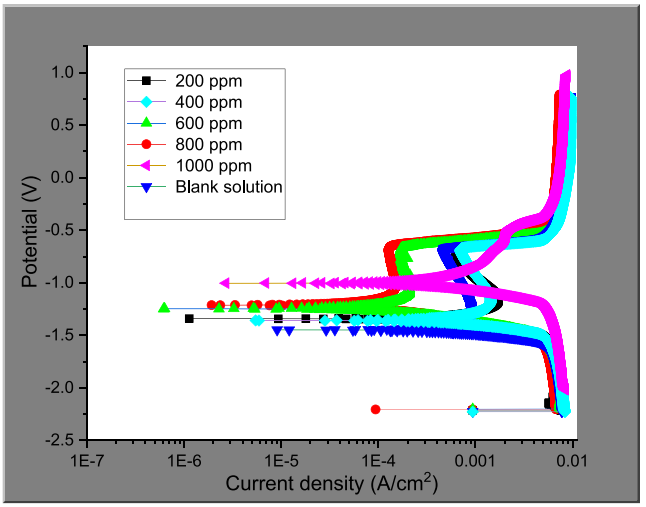

Figure 1. Potential−current curve for aluminum in the 3.5 wt % NaCl with and without diverse concentration of PEO (T = 298 K and sweep rate = 0.2 mV/s).

associated corrosion kinetics parameters, corrosion potential (E_{corr}), current density (i_{corr}), cathodic and anodic Tafel slope (βc and βa), and the corresponding CR are presented in Table 1. Figure 1 demonstrates that in the presence of PEO, the corrosion current values considerably decreased with no changes in the polarization curve shape suggesting that the inhibition of PEO blocks the active site present on the aluminum surface with no changes to the corrosion mechanisms.[34,35] This behavior implies that the PEO does not affect the cathodic and anodic reaction mechanisms but changes the CRs. As shown in Table 1, increased PEO was linked to the active coverage sites that reduced the rate of corrosion and controlled both the hydrogen evolution in the system and the oxidation dissolution of the metal,[36,37] through

https://doi.org/10.1021/acsomega.2c00540
ACS Omega 2022, 7, 40740−40749

Table 1. Potentiodynamic Polarization Parameter for Aluminum in the 3.5 wt % NaCl with and without Diverse Concentrations of PEO

system (3.5% NaCl) (ppm PEO)	E_{corr}(V)	i_{corr}(A/cm^2)	CR (mm/year)	polarization resistance (Ω)	βa (V/dec)	βc (V/dec)	inhibition efficiency (%)
0.0	−1.4503	0.0006206	7.2116	57.046	0.2074	0.0550	
200	−1.3741	0.0003277	3.8074	57.660	1.3588	0.4497	90.86
400	−1.3602	0.0002119	2.4619	73.140	0.1023	0.0382	92.88
600	−1.3435	0.0001886	2.1909	236.430	0.0697	0.0583	97.27
800	−1.2495	1.7344E-05	0.2015	429.020	0.0236	0.0185	97.92
1000	−1.2145	1.0515E-05	0.1222	579.220	0.0057	0.0388	98.37

the electron lone-pairs from PEO and formation of complexes from aluminum cations. The result further denotes that utmost E_{corr} value displacement for inhibited samples to uninhibited samples was below 85 mV, signifying that PEO behaves as a mixed-type corrosion inhibitor.[38] The CR value of the exposed specimen to 1000 ppm PEO solutions was observed to decrease significantly from 7.2116 to 0.1222 mm/year. This may be due to the compact inhibitor films formed on the metal surface, which results in blocking the process of corrosion. Furthermore, this specimen illustrates a noticeable increase of the polarization value to 579.22 (Ω). The decreased CR and increased polarization value at increased inhibitor concentration could be ascribed to the increased double layer thickness owing to the complex compound formed in the solution/metal interface.[39] This result shows the high capability of PEO in reducing the aluminum CR via film formation and/or adsorption on the active sites. In conformity with the EIS result, the polarization parameter showed that 1000 ppm PEO offered the highest corrosion inhibition performance.

3.1.2. EIS Study. The EIS tests were conducted in the 3.5% sodium chloride media to verify the potentiodynamic polarization result and to understand the corrosion performance of PEO better. The Nyquist corrosion plots (Figure 2) for samples in the 3.5% sodium chloride medium show that the Nyquist plot diameter is higher in the presence of PEO compared to the uninhibited sample. The Nyquist plot shows that the immersed samples in the NaCl solutions with PEO displayed large semicircles compared with the sample in the blank solutions, signifying the inhibitive performance of PEO.

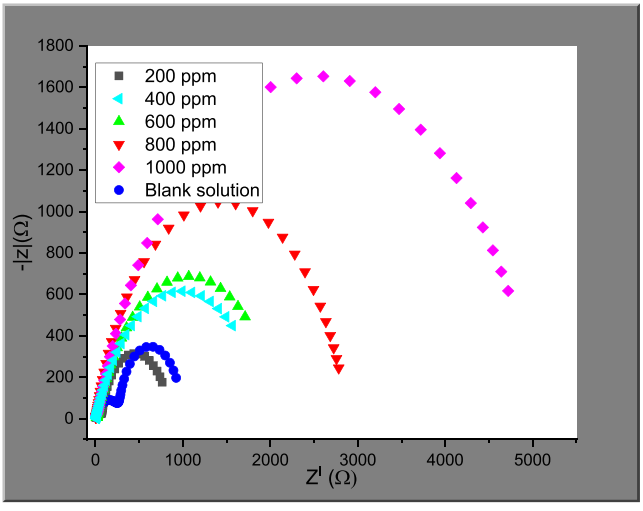

Figure 2. Nyquist plots for aluminum in the 3.5 wt % NaCl solution without and with various concentrations of PEO at (T = 298 K).

The plot does not show perfect semicircles because of the surface inhomogeneity and frequency dispersion.[40] The sample with 1000 ppm Nyquist' semicircle diameter was observed to be much greater than the other concentrations indicating that 1000 ppm concentration gives better corrosion protection for the aluminum sample in the chloride solution. Also, the Nyquist plot diameter increases with inhibitor concentrations. The difference between real impedance at higher and low frequencies is mainly known as the charge transfer resistances (R_{ct}) during Nyquist plot interpretation. However, it is evident that corroding metal in chloride solutions with the inhibitor is mainly linked with several resistances such as diffusion layer resistance (R_d), resistance owing to corrosion product accumulation, that is, accumulation resistance (R_a), and resistance due to the inhibitor film, that is, film resistance (R_f). Thus, in this study, polarization resistance ($R_p = R_d + R_a + R_f$) was studied instead of charge transfer resistance (R_{ct}). The Nyquist plots show the transition of the capacitive loop (CL) to the inductive loop in the lower frequency region, because of the relaxation process of the adsorbates, resulting from the property of the sodium chloride film modulation of the electrochemical reaction, dissolved aluminum ion adsorption on the interface, and formation of the two-stage faradaic process of desorption-adsorption of the adsorbate in previous passive potential regions. Better estimation was noticed with replacement of capacitance by the constant phase element (CPE) for metal dissolution in chloride solutions. The CPE impedance can be represented with eq 4:

$$Z_{CPE} = \left(\frac{1}{Y_0}\right)[(j\omega)^n]^{-1} \quad (4)$$

where Y_0 is the CPE constant; j represents the imaginary number; n is the phase shift which measures the surface homogeneity; and ω denotes the angular frequency.

Generally, a high phase shift value denotes the high smoothness of the surface. The phase shifts also explain the CPE nature as n = 0 denotes resistor, n = 0.5 signifies Warburg impedance, n = −1 represents inductance, and n = 1 represents capacitance. The EIS data show that n values in this study vary between 0.800 and 0.807 signifying that the CPE performs as capacitances. Deviating from n = 1 (ideal capacitive performance) is ascribed to the inhomogeneity of the surface. The time constant with low impedance for aluminum normally denotes the formation of corrosion products on the surface of the metal.[41] It is observed that the R_p value increased while the C_{dl} value decreases with increasing the PEO concentrations, this observation denotes that the PEO inhibits the aluminum against corrosion via adsorption on the aluminum/electrolyte interfaces. The PEO adsorption behavior on the aluminum/electrolyte interface was investigated further by the Bode plot (Figure 3). This type of deviation again could be attributed to

https://doi.org/10.1021/acsomega.2c00540
ACS Omega 2022, 7, 40740−40749

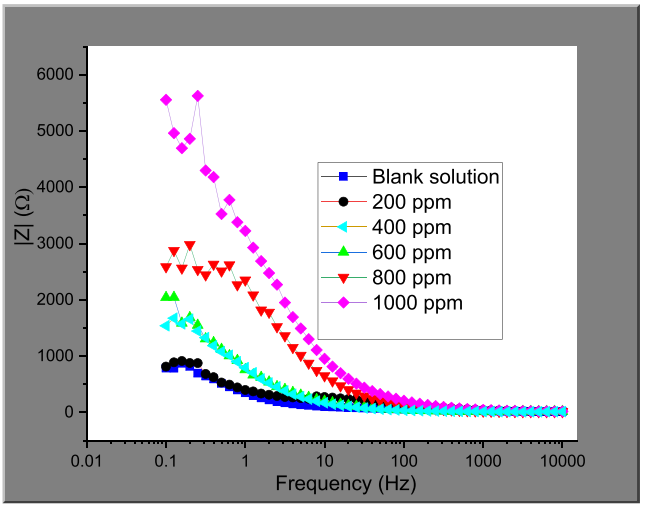

Figure 3. Bode plot for aluminum in the 3.5 wt % NaCl solution without and with various concentrations of PEO at (T = 298 K).

surface inhomogeneity owing to the structural and interfacial origin. This figure shows an increased linear slope section as PEO increased denoting the existence of PEO on the aluminum surface, before the slide oxidation. An increase in the phase angle (Figure 4) implies better performance of

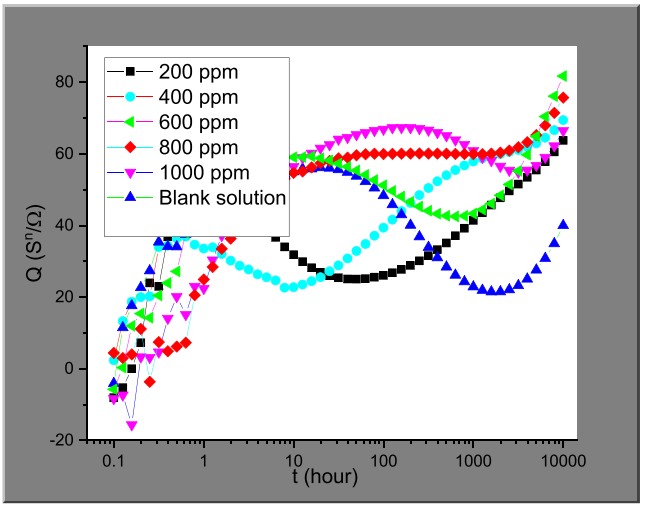

Figure 4. Phase angle plot for aluminum in the 3.5 wt % NaCl solutions with and without various concentrations of PEO at (T = 298 K).

PEO.[42] The higher CLs imply PEO adsorption rather than desorption. However, in the present case, the uninhibited sample shows a slight decrease in frequency impedance with exposure time and the corresponding phase angle plateau at high frequencies decreased. This observation may be ascribed to the initiation of corrosion and slow corrosion products formed on the aluminum surface, giving some level of protection for the aluminum dissolution. It appears that more inhibiting species is available at the aluminum surface-active zone with higher PEO concentration. This denotes that adding 1000 ppm PEO to the aggressive solution results in high corrosion inhibitive behavior. The high negative phase angles at higher frequency of the inhibited specimen with 1000 ppm PEO also prove better corrosion inhibition compared with other specimens, denoting the high capacitive performance of this system. The significant difference in the result derived from the EIS measurement suggests that the highest level of inhibitive behavior was achieved at 1000 ppm PEO. The higher inhibitive behavior at this concentration could be linked to the high inhibitive component value, suggesting that a large number of inhibitive components existing in the chloride solution resulted in a higher corrosion inhibition property on the aluminum surface thereby blocking the aggressive ion path interference to the aluminum surface.

3.2. Weight Loss Tests. The weight loss results for aluminum in 3.5% NaCl solution are presented in Figures 5

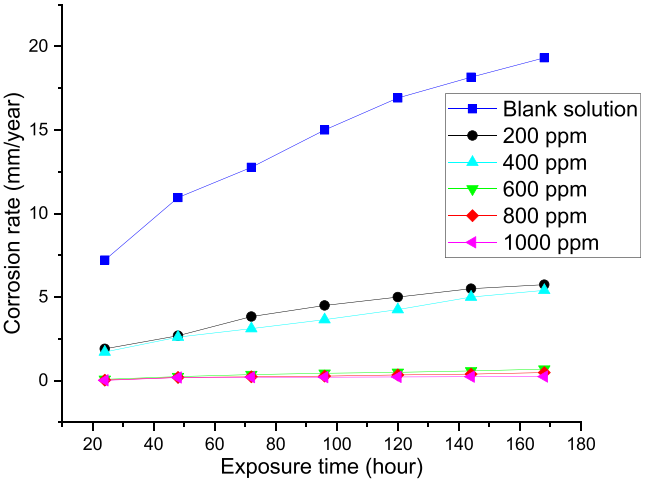

Figure 5. CR vs exposure time for aluminum corrosion in the 3.5 wt % NaCl solutions with and without various concentrations of PEO at (T = 298 K).

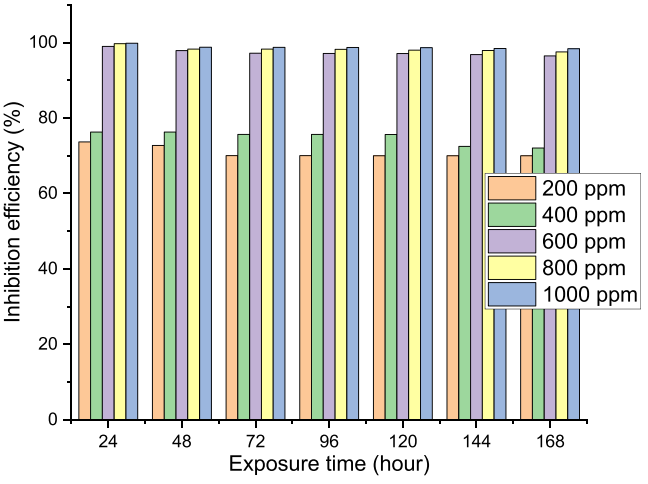

Figure 6. Inhibition efficiency vs exposure time for aluminum corrosion in the 3.5 wt % NaCl solution without and with different concentrations of PEO at (T = 298 K).

and 6. A sharp increase in the CR value was noticed with exposure time. However, the CR value reduced with the addition of PEO. Because a low CR denotes high inhibitor efficiency, Figure 6 affirms that the increase in PEO concentration led to improved efficiency. An inhibition efficiency value of 97.01% was achieved at 298 °K with 1000

https://doi.org/10.1021/acsomega.2c00540
ACS Omega 2022, 7, 40740−40749

ppm PEO but decreased steadily with exposure time. Observation of this result shows that the inhibitive tendency of PEO increases with concentration. The results also denote that the increase in PEO concentration from 600 to 1000 ppm did not cause notable changes in the inhibition behavior indicating 600 ppm as the optimum concentration. The high inhibitive behavior of PEO is ascribed to the presence of different heteroatoms for instance N and O and a high carbon skeleton by which they can efficiently adsorbed on the aluminum surface. The obtained result revealed that the inhibitive efficiency of PEO decreases from 97.01 to 96.03% with exposure time from 24 to 168 h. This behavior is attributed primarily to increased inhibitor kinetic energy, as exposure time increases which in turn decreases the force of attraction between the PEO and aluminum surface.

3.3. Effect of Inhibitor Concentrations and Adsorption Isotherms. For this study, the corrosion inhibition equation is

$$PEO_{sol} + xH_2O_{ads} \rightarrow PEO_{ads} + xH_2O_{sol} \quad (5)$$

where PEO_{sol} is the PEO in the solution, PEO_{ads} is the PEO adsorbates on the aluminum surface, and x is the quantity of initial water molecules attached to the aluminum, before displacement.[43] To explain the PEO adsorption behavior on the aluminum surface, different isotherms, for example, Freundlich, Frumkin, Langmuir, and Temkin isotherms were studied, and the Langmuir adsorption isotherm showed the best fit. Freundlich, Langmuir, and Temkin adsorption models shown in eqs 6 and 7 were fitted respectively to study the reaction thermodynamics taking place during corrosion of aluminum.

$$\frac{C_{PEO}}{A} = \frac{1}{K_{ads}} + C_{PEO} \quad (6)$$

$$A = \left(-\frac{1}{2b}\right)\ln K_{ads} + \left(-\frac{1}{2b}\right)C_{PEO} \quad (7)$$

where K_{ads} is the adsorption equilibrium coefficient, C_{PEO} is inhibitor concentration, and b is the sign-dependent parameter, respectively. The Gibbs free energy adsorption and the equilibrium coefficient adsorption are related by eq 8.

$$\Delta G^{\circ}_{ads} = RT\ln 1000K_{ads} \quad (8)$$

The regression coefficient value (R^2) was used as the criterion for selecting the most excellent isotherms. It is significant to state that the R^2 value was close to unity for Langmuir adsorption isotherms (R^2 = 0.9872; Figure 7); nevertheless, the slope value deviates from an ideal Langmuir adsorption isotherm performance as the value is apart from unity. This observation could be ascribed to the intermolecular interaction between inhibitor molecules adsorbed and the energy change aluminum surface that is not measured during the Langmuir isotherm formula formulation.[44] The regression coefficients increased in the order: Langmuir, Temkin, and Freundlich. Langmuir and Freundlich showed involvement of physical adsorption, via the attraction of PEO charged hydrophilic groups on the aluminum surface. This was further confirmed by the increase in Langmuir adsorption equilibrium constant ($K_{adsorption}$) values shown in Table 2. The low efficiency obtained after 198 h exposure in the solutions containing 200 ppm PEO compared to the 1000 ppm PEO solution value could be ascribed to thicker inhibitor films

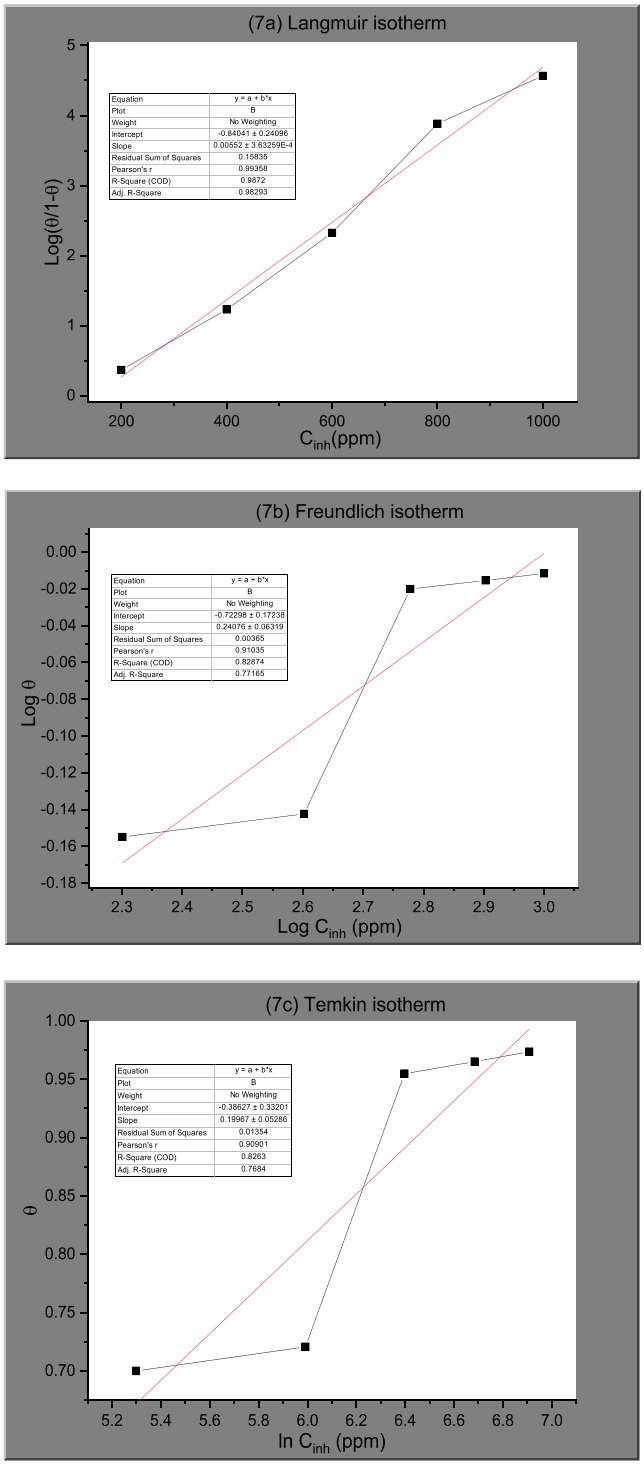

Figure 7. (a) Langmuir, (b) Freundlich, and (c) Temkin isotherms of PEO in 3.5% NaCl solutions.

adsorbed on the aluminum surface. This behavior could also indicate the steady water molecule replacement by the inhibitor molecule that forms defensive layers at the aluminum/solution interface.

3.4. Surface Analysis. The scanning electron microscopy (SEM) micrograph for aluminum after 168 h exposure time in the sodium chloride solution with and without PEO is represented in Figure 8. For the uninhibited sample (Figure 8a), there is evident surface roughness with corrosion products

https://doi.org/10.1021/acsomega.2c00540
ACS Omega 2022, 7, 40740−40749

Table 2. Adsorption Parameters on Aluminum Corrosion Inhibition by PEO Obtained from the Langmuir, Freundlich, and Temkin Adsorption Isotherm

inhibitor system	adsorption isotherms					
	Langmuir		Freundlich		Temkin	
	$K_{adsorpion}$	R^2	$K_{adsorpion}$	R^2	$K_{adsorpion}$	R^2
Al + PEO + 3.5%NaCl solutions	7.2500	0.9872	2.5100	0.8287	2.2300	0.8263

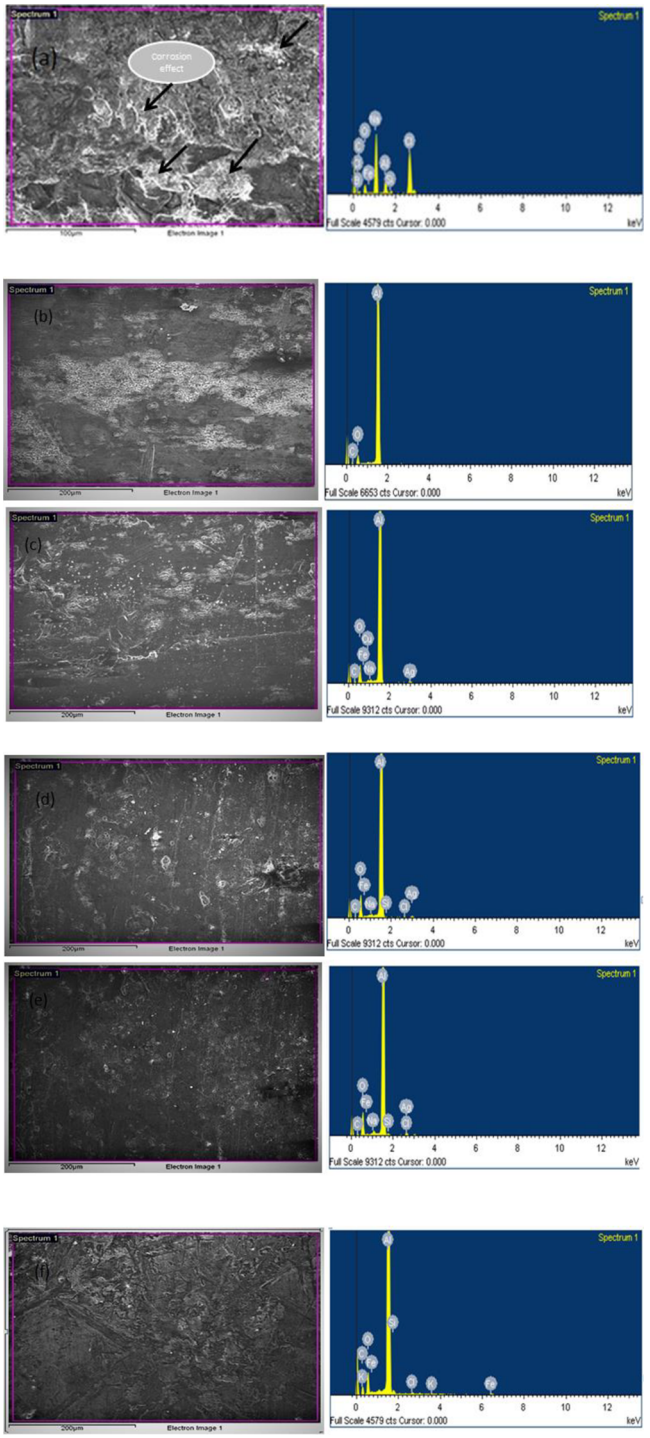

Figure 8. SEM micrographs for aluminum, after 168 h of immersion in 3.5% NaCl solution (a) without PEO (b) with 200 ppm PEO, (c) with 400 ppm PEO, (d) with 600 ppm PEO, (e) with 800 ppm PEO, and (f) with 1000 ppm PEO.

on the metal surface, owing to its direct contact with the aggressive solutions. This observation denotes that the uninhibited aluminum surface is highly corroded. However, a smooth surface was observed with the addition of an inhibitor (Figure 8b–f) validating the Tafel, EIS, and weight loss results. The SEM observations show that there was an inhibitive film on the surface of the aluminum that showed low permeability for the corrosive ions and protected the aluminum from corrosion. EDX analysis was conducted on the uninhibited and inhibited samples to study the elemental compositions on the aluminum surface after 168 h of exposure to 3.5% NaCl solution. The surface analysis of the uninhibited sample shows that Na, Cl, Al, and O were detected, with high Cl and Na and lower Al. The spectra show additional lines indicating the existence of C, Si, and C, relating to general anodic attack obscuring the underlying metal surface.[45] The sample with PEO shows very thin nodular oxides signifying minimal corrosion attacks. This observation supports the EIS findings that suggest inhomogeneity organic films on the aluminum surface. The EDX analysis demonstrated the presence of a minute amount of chloride in the inhibited samples (Figure 8b–f) compared with the uninhibited sample (Figure 8a) owing to the micropores, which make a path for the penetration of corrosive ions, including chloride. The 1000 ppm sample registered the lowest chloride content in comparison to the other concentrations. The reduction of Cl content confirms that the presence of inhibitor provides improved anticorrosion properties, suggesting that the PEO blocks the surface of the metal from Cl attacks on the aluminum surface. This conformed with the result previously reported,[31] and this may be ascribed to the adsorbed inhibitive component on the surface of the aluminum protecting it from corrosion. Because the addition of the inhibitor gives the lowest chloride content, it suggests that incorporating PEO offers efficient adsorption onto the metal substrate. These variations in the value of atoms in the absence and presence of an inhibitor help to understand the changes caused by the formation of a protective layer.[45]

3.5. Corrosion Mechanism. The oxygen reduction reaction directs the aluminum cathode process (eq 9) in aerated sodium chloride solution, that is, the electron acceptor reactions from the metal oxidation (eq 10);

$$O_2 + 2H_2O + 4e^- \rightarrow 4OH^- \quad (9)$$

$$Al \rightarrow 3e^- + Al^{3+} \quad (10)$$

Aluminum matrix dissolution in chloride solution occurs via a sequence of oxidation reactions,

producing the $Al(OH)Cl^+$ complex that dissolved in aqueous media[47] following eq 11 to eq 17;

$$Al + 3H_2O \rightarrow Al(OH)_3 + 3H^+ + 3e^- \quad (11)$$

$$Al + 2H_2O \rightarrow AlO(OH) + 3H^+ + 3e^- \quad (12)$$

https://doi.org/10.1021/acsomega.2c00540
ACS Omega 2022, 7, 40740−40749

$$Al + \frac{3}{2}H_2O \rightarrow Al_2O_3 + 3H^+ + 3e^- \quad (13)$$

$$Al(OH)^{2+} + Cl^- \rightarrow Al(OH)Cl^+3H^+ + 3e^- \quad (14)$$

Efficient inhibitors stop or hinder both or one of the cathodic and anodic reactions. In the case of corrosion inhibition by PEO, two corrosion prevention mechanisms are suggested:

(i) The first mechanism is that the compound is formed through vacant orbitals and the organic component in PEO. In this mechanism, the compound is adsorbed on the aluminum to obstruct the anodic and cathodic reactions. In this scenario, the PEO is considered to be mixed type.

(ii) The reduction reaction is the second mechanism (eq 15). The assumption that the anodic reaction is aluminum matrix oxidation (eq 16) is acceptable. The formed inhibitors react to form thin hydroxide layers (eq 17). The thin PEO layers do not appear to be adequate in achieving corrosion protection by cathodic reaction inhibition. Therefore, the cathodic type inhibitor is predominant in this case.

$$PEO + OH^- \rightarrow PEO(OH) \quad (15)$$

$$O_2 + H_2O + 2e^- \rightarrow H_2O_2 + OH^- \quad (16)$$

$$PEO + H_2O_2 \rightarrow PEO^{2+} + 2OH^- \quad (17)$$

The two mechanisms are the predominant and valid mechanisms that may depend on the total inhibitor concentrations. Also, the Tafel result showed that PEO is a mixed-type. Thus, the first mechanism for preventing corrosion, discussed above, appears to be the main mechanism. In this study, from the weight loss, potentiodynamic polarization test, electrochemical impedance spectroscopy, and SEM/EDX tests, we can conclude that the PEO is responsible for the formed protective multi or monolayers on the surface of the aluminum with no preferential deposition.

4. CONCLUSIONS

The corrosion inhibition tendency of parsley essential oil as a cheap sustainable inhibitor for aluminum in 3.5% NaCl media was shown by weight loss analysis, EIS, potentiodynamic polarization, and the SEM/EDX technique. The EIS analysis validates that the PEO mitigates the aluminum corrosion via adsorption at the electrolyte/aluminum interface and thus forms protective layers on the aluminum surface. The corrosion inhibitive behavior significantly increased as the inhibitor concentration increased; 97.01% efficiency was achieved after 24 h of immersion with 1000 ppm inhibitor concentration. The obtained results from weight loss analysis, EIS, potentiodynamic polarization, and morphological characterization were in good agreement. The spontaneous PEO adsorption on the aluminum surface was examined with Langmuir, Freundlich, and Temkin adsorption isotherms. Polarization results showed that PEO restrained the corrosion effectively and classified it as the mixed-type corrosion inhibitor. The PEO adsorption on the aluminum surface was further supported by the SEM and EDX test where noticeable surface smoothness was observed with the inhibitor.

AUTHOR INFORMATION

Corresponding Authors

Omotayo Sanni − *Department of Chemical Engineering, Faculty of Engineering, Built Environment and Information Technology, University of Pretoria, Pretoria 0028, South Africa*; Email: tayo.sanni@yahoo.com

Michael O. Daramola − *Department of Chemical Engineering, Faculty of Engineering, Built Environment and Information Technology, University of Pretoria, Pretoria 0028, South Africa*; orcid.org/0000-0003-1475-0745; Email: michael.daramola@up.ac.za

Author

Samuel A. Iwarere − *Department of Chemical Engineering, Faculty of Engineering, Built Environment and Information Technology, University of Pretoria, Pretoria 0028, South Africa*

Complete contact information is available at: https://pubs.acs.org/10.1021/acsomega.2c00540

Notes

The authors declare no competing financial interest.

REFERENCES

(1) Mishra, R. Study the effect of pre-corrosion on mechanical properties and fatigue life of aluminum alloy 8011. *Mater. Today: Proc.* **2020**, *25*, 602−609.

(2) Luo, C.*Role of microstructure on corrosion control of AA2024-T3 aluminium alloy*; University of Manchester. Manchester: Faculty of Engineering and Physical Sciences. 2011.

(3) Liew, Y.; Örnek, C.; Pan, J.; Thierry, D.; Wijesinghe, S.; Blackwood, D. J. Towards understanding micro-galvanic activities in localised corrosion of AA2099 aluminium alloy. *Electrochim. Acta* **2021**, *392*, No. 139005.

(4) Ormellese, M.; Lazzari, L.; Goidanich, S.; Fumagalli, G.; Brenna, A. A study of organic substances as inhibitors for chloride-induced corrosion in concrete. *Corros. Sci.* **2009**, *51*, 2959−2968.

(5) Hu, R. G.; Zhang, S.; Bu, J. F.; Lin, C. J.; Song, G. L. Recent progress in corrosion protection of magnesium alloys by organic coatings. *Prog. Org. Coat.* **2012**, *73*, 129−141.

(6) Kendig, M.; Jeanjaquet, S.; Addison, R.; Waldrop, J. Role of hexavalent chromium in the inhibition of corrosion of aluminum alloys. *Surf. Coat. Technol.* **2001**, *140*, 58−66.

(7) Pokorny, P.; Tej, P.; Szelag, P. Chromate conversion coatings and their current application. *Metalurgija* **2016**, *55*, 253−256.

(8) Kumar, L.; Bharadvaja, N.Microbial remediation of heavy metals. *Microbial Bioremediation & Biodegradation*. 2020, 49−72.

(9) Weiss, E. J.*Preliminary ecological risk assessment to assess the implications of replacing chromium plating with tantalum coating*. 1999.

(10) Ayele, A.; Godeto, Y. G. Bioremediation of chromium by microorganisms and its mechanisms related to functional groups. *J. Chem.* **2021**, *2021*, No. 7694157.

(11) Guo, L.; Obot, I. B.; Zheng, X.; Shen, X.; Qiang, Y.; Kaya, S.; Kaya, C. Theoretical insight into an empirical rule about organic corrosion inhibitors containing nitrogen, oxygen, and sulfur atoms. *Appl. Surf. Sci.* **2017**, *406*, 301−306.

(12) Assad, H.; Kumar, A. Understanding functional group effect on corrosion inhibition efficiency of selected organic compounds. *J. Mol. Liq.* **2021**, *344*, No. 117755.

(13) Verma, C.; Verma, D. K.; Ebenso, E. E.; Quraishi, M. A. Sulfur and phosphorus heteroatom-containing compounds as corrosion inhibitors: An overview. *Heteroat. Chem.* **2018**, *29*, No. e21437.

(14) Ghailane, T.; Balkhmima, R. A.; Ghailane, R.; Souizi, A.; Touir, R.; Ebn Touhami, M.; Marakchi, K.; Komiha, N. Experimental and theoretical studies for mild steel corrosion inhibition in 1 M HCl by two new benzothiazine derivatives. *Corros. Sci.* **2013**, *76*, 317−324.

https://doi.org/10.1021/acsomega.2c00540
ACS Omega 2022, 7, 40740−40749

(15) Verma, D. K.; Dewangan, Y.; Dewangan, A. K.; Asatkar, A. Heteroatom-based compounds as sustainable corrosion inhibitors: an overview. *J. Bio- Tribo-Corros.* **2021**, *7*, 1−18.
(16) Barbouchi, M.; Benzidia, B.; Aouidate, A.; Ghaleb, A.; el Idrissi, M.; Choukrad, M.'. Theoretical modeling and experimental studies of Terebinth extracts as green corrosion inhibitor for iron in 3% NaCl medium. *J. King Saud Univ. Sci.* **2020**, *32*, 2995−3004.
(17) Dhouibi, I.; Masmoudi, F.; Bouaziz, M.; Masmoudi, M. A study of the anti-corrosive effects of essential oils of rosemary and myrtle for copper corrosion in chloride media. *Arab. J. Chem.* **2021**, *14*, No. 102961.
(18) Bammou, L.; Chebli, B.; Salghi, R.; Bazzi, L.; Hammouti, B.; Mihit, M.; Idrissi, H. Thermodynamic properties of Thymus satureioides essential oils as corrosion inhibitor of tinplate in 0.5 M HCl: chemical characterization and electrochemical study. *Green Chem. Lett. Rev.* **2010**, *3*, 173−178.
(19) Halambek, J.; Berković, K.; Vorkapić-Furač, J. Laurus nobilis L. oil as green corrosion inhibitor for aluminium and AA5754 aluminium alloy in 3% NaCl solution. *Mater. Chem. Phys.* **2013**, *137*, 788−795.
(20) Zakir Hossain, S. M.; Kareem, S.; Alshater, A.; Alzubair, H.; Razzak, S.; Hossain, M. Effects of cinnamaldehyde as an eco-friendly corrosion inhibitor on mild steel in aerated NaCl solutions. *Arab. J. Sci. Eng.* **2020**, *45*, 229−239.
(21) Cissé, K.; Gassama, D.; Thiam, A.; Bathily, M.; Fall, M. Evaluation of the inhibitory effectiveness of cyperus articulatus essential oils on the corrosion of structural steelwork in hydrochloric acid solution. *Chem. Afr.* **2021**, *4*, 379−390.
(22) Dahmani, K.; Galai, M.; Ouakki, M.; Cherkaoui, M.; Touir, R.; Erkan, S. U. L. T. A. N.; Kaya, S.; el Ibrahimi, B. Quantum chemical and molecular dynamic simulation studies for the identification of the extracted cinnamon essential oil constituent responsible for copper corrosion inhibition in acidified 3.0 wt% NaCl medium. *Inorg. Chem. Commun.* **2021**, *124*, No. 108409.
(23) Chraka, A.; Raissouni, I.; Benseddik, N.; Khayar, S.; Ibn Mansour, A.; Belcadi, H.; Chaouket, F.; Bouchta, D. Aging time effect of Ammi visnaga (L.) lam essential oil on the chemical composition and corrosion inhibition of brass in 3% NaCl medium. Experimental and theoretical studies. *Mater. Today: Proc.* **2020**, *22*, 83−88.
(24) Ji, G.; Shukla, S. K.; Dwivedi, P.; Sundaram, S.; Ebenso, E. E.; Prakash, R. Parthenium hysterophorus plant extract as an efficient green corrosion inhibitor for mild steel in acidic environment. *Int. J. Electrochem. Sci.* **2012**, *7*, 9933−9945.
(25) Obot, I. B.; Obi-Egbedi, N. O. An interesting and efficient green corrosion inhibitor for aluminium from extracts of Chlomolaena odorata L. in acidic solution. *J. Appl. Electrochem.* **2010**, *40*, 1977−1984.
(26) Okafor, P. C.; Ebenso, E. E.; Ekpe, U. J. Azadirachta indica extracts as corrosion inhibitor for mild steel in acid medium. *Int. J. Electrochem. Sci.* **2010**, *5*, 978−993.
(27) Nnanna, L. A.; Uchendu, K. O.; Nwosu, F. O.; Ihekoronye, U.; Eti, P. Gmelina Arborea Bark Extracts as a Corrosion Inhibitor for mild steel in an acidic environment. *Int. J. Mater. Chem.* **2014**, *4*, 34−39.
(28) Salehi, E.; Naderi, R.; Ramezanzadeh, B. Synthesis and characterization of an effective organic/inorganic hybrid green corrosion inhibitive complex based on zinc acetate/Urtica Dioica. *Appl. Surf. Sci.* **2017**, *396*, 1499−1514.
(29) Sanaei, Z.; Shahrabi, T.; Ramezanzadeh, B. Synthesis and characterization of an effective green corrosion inhibitive hybrid pigment based on zinc acetate-Cichorium intybus L leaves extract (ZnA-CIL. L): Electrochemical investigations on the synergistic corrosion inhibition of mild steel in aqueous chloride solutions. *Dyes Pigm.* **2017**, *139*, 218−232.
(30) Sanni, O.; Popoola, A.; Fayomi, O. Corrosion inhibition comparison of the effect of green inhibitor on the corrosion behavior of 316L and 904L austenitic stainless steels in chloride environment. *J. Phys.: Conf. Ser.* **2019**, *1378*, No. 022087.
(31) Garcia, S. J.; Markley, T. A.; Mol, J. M. C.; Hughes, A. E. Unravelling the corrosion inhibition mechanisms of bi-functional inhibitors by EIS and SEM−EDS. *Corros. Sci.* **2013**, *69*, 346−358.
(32) Astm, G. G.*31-72: Standard Practice for Laboratory Immersion Corrosion Testing of Metals*; Annual Book of Standards2004.
(33) Sanni, O.; Popoola, A. P. I. Data on environmental sustainable corrosion inhibitor for stainless steel in aggressive environment. *Data Brief* **2019**, *22*, 451−457.
(34) Li, S.-M.; Zhang, H.-R.; Liu, J.-H. Corrosion behavior of aluminum alloy 2024-T3 by 8-hydroxy-quinoline and its derivative in 3.5% chloride solution. *Trans. Nonferrous Met. Soc. China* **2007**, *17*, 318−325.
(35) Lamaka, S. V.; Zheludkevich, M. L.; Yasakau, K. A.; Montemor, M. F.; Ferreira, M. G. S. High effective organic corrosion inhibitors for 2024 aluminium alloy. *Electrochim. Acta* **2007**, *52*, 7231−7247.
(36) Oguzie, E. E. Corrosion inhibition of aluminium in acidic and alkaline media by Sansevieria trifasciata extract. *Corros. Sci.* **2007**, *49*, 1527−1539.
(37) Obot, I. B.; Obi-Egbedi, N. O.; Umoren, S. A. The synergistic inhibitive effect and some quantum chemical parameters of 2, 3-diaminonaphthalene and iodide ions on the hydrochloric acid corrosion of aluminium. *Corros. Sci.* **2009**, *51*, 276−282.
(38) Loto, R. T.; Loto, C. A.; Popoola, A. P. Inhibition effect of deanol on mild steel corrosion in dilute sulphuric acid. *S. Afr. J. Chem.* **2015**, *68*, 105−114.
(39) Lgaz, H.; Chung, I.-M.; Albayati, M. R.; Chaouiki, A.; Salghi, R.; Mohamed, S. K. Improved corrosion resistance of mild steel in acidic solution by hydrazone derivatives: An experimental and computational study. *Arab. J. Chem.* **2020**, *13*, 2934−2954.
(40) Döner, A.; Kardaş, G. N-Aminorhodanine as an effective corrosion inhibitor for mild steel in 0.5 M H_2SO_4. *Corros. Sci.* **2011**, *53*, 4223−4232.
(41) Wysocka, J.; Krakowiak, S.; Ryl, J. Evaluation of citric acid corrosion inhibition efficiency and passivation kinetics for aluminium alloys in alkaline media by means of dynamic impedance monitoring. *Electrochim. Acta* **2017**, *258*, 1463−1475.
(42) Qiang, Y.; Fu, S.; Zhang, S.; Chen, S.; Zou, X. Designing and fabricating of single and double alkyl-chain indazole derivatives self-assembled monolayer for corrosion inhibition of copper. *Corros. Sci.* **2018**, *140*, 111−121.
(43) Udensi, S. C.; Ekpe, O. E.; Nnanna, L. A. Corrosion inhibition performance of low cost and eco-friendly Treculia africana leaves extract on aluminium alloy AA7075-T7351 in 2.86% NaCl solutions. *Sci. Afr.* **2021**, *12*, No. e00791.
(44) Verma, C.; Quraishi, M. A.; Kluza, K.; Makowska-Janusik, M.; Olasunkanmi, L. O.; Ebenso, E. E. Corrosion inhibition of mild steel in 1M HCl by D-glucose derivatives of dihydropyrido [2, 3-d: 6, 5-d′] dipyrimidine-2, 4, 6, 8 (1H, 3H, 5H, 7H)-tetraone. *Sci. Rep.* **2017**, *7*, 44432.
(45) Hou, L.; Li, Y.; Sun, J.; Zhang, S. H.; Wei, H.; Wei, Y. Enhancement corrosion resistance of MgAl layered double hydroxides films by anion-exchange mechanism on magnesium alloys. *Appl. Surf. Sci.* **2019**, *487*, 101−108.
(46) Chung, I. M.; Malathy, R.; Kim, S. H.; Kalaiselvi, K.; Prabakaran, M.; Gopiraman, M. Ecofriendly green inhibitor from Hemerocallis fulva against aluminum corrosion in sulphuric acid medium. *J. Adhes. Sci. Technol.* **2020**, *34*, 1483−1506.
(47) Gobara, M.; Baraka, A.; Akid, R.; Zorainy, M. Corrosion protection mechanism of Ce^{4+}/organic inhibitor for AA2024 in 3.5% NaCl. *RSC Adv.* **2020**, *10*, 2227−2240.
(48) Abdallah, M.; Altass, H. M.; Al-Gorair, A. S.; Al-Fahemi, J. H.; Jahdaly, B. A. A. L.; Soliman, K. A. Natural nutmeg oil as a green corrosion inhibitor for carbon steel in 1.0 M HCl solution: Chemical, electrochemical, and computational methods. *J. Mol. Liq.* **2021**, *323*, No. 115036.
(49) Tongnuanchan, P.; Benjakul, S.; Prodpran, T. Properties and antioxidant activity of fish skin gelatin film incorporated with citrus essential oils. *Food Chem.* **2012**, *134*, 1571−1579.

https://doi.org/10.1021/acsomega.2c00540
ACS Omega 2022, 7, 40740−40749

(50) Tongnuanchan, P.; Benjakul, S. Essential oils: extraction, bioactivities, and their uses for food preservation. *J. Food Sci.* **2014**, *79*, R1231−R1249.
(51) Zheng, G. Q.; Kenney, P. M.; Zhang, J.; Lam, L. K. T. Inhibition of benzo [a] pyrene-induced tumorigenesis by myristicin, a volatile aroma constituent of parsley leaf oil. *Carcinogenesis* **1992**, *13*, 1921−1923.
(52) Tauferova, A.; Pospiech, M.; Javurkova, Z.; Tremlova, B.; Dordevic, D.; Jancikova, S.; Tesikova, K.; Zdarsky, M.; Vitez, T.; Vitezova, M. Plant Byproducts as part of edible coatings: A case study with parsley, grape and blueberry pomace. *Polymer* **2021**, *13*, 2578.

https://doi.org/10.1021/acsomega.2c00540
ACS Omega 2022, 7, 40740−40749